Available online at www.sciencedirect.com
ScienceDirect
Journal of the European Ceramic Society 29 (2009) 3177–3184
www.elsevier.com/locate/jeurceramsoc

Hot pressed and spark plasma sintered zirconia/carbon nanofiber composites

Ján Dusza [a,*], Gurdial Blugan [b], Jerzy Morgiel [c], Jakob Kuebler [b], Fawad Inam [d], Ton Peijs [d], Michael J. Reece [d], Viktor Puchy [a]

[a] *Institute of Materials Research, Slovak Academy of Sciences, Watsonova 47, 04353 Košice, Slovak Republic*
[b] *Empa, Swiss Federal Laboratories for Materials Testing and Research, Laboratory for High Performance Ceramics, 8600 Duebendorf, Switzerland*
[c] *Institute of Metellurgy and Materials Science of Polish Academy of Sciences, Reymonta 25, 30 059 Krakow, Poland*
[d] *Nanoforce Technology Ltd. and Centre for Materials Research, Queen Mary University of London, Mile End Road, London, UK*

Received 27 March 2009; received in revised form 7 May 2009; accepted 25 May 2009
Available online 26 June 2009

Abstract

Zirconia/carbon nanofiber composites were prepared by hot pressing and spark plasma sintering with 2.0 and 3.3 vol.% of carbon nanofibers (CNFs). The effects of the sintering route and the carbon nanofiber additions on the microstructure, fracture/mechanical and electrical properties of the CNF/3Y-TZP composites were investigated. The microstructure of the ZrO_2 and ZrO_2–CNF composites consisted of a small grain sized matrix (approximately 120 nm), with relatively well dispersed carbon nanofibers in the composite. All of the composites showed significantly higher electrical conductivity (from 391 to 985 S/m) compared to the monolithic zirconia (approximately 1×10^{-10} S/m). The spark plasma sintered composites exhibited higher densities, hardness and indentation toughness but lower electrical conductivity compared to the hot pressed composites. The improved electrical conductivity of the composites is caused by CNFs network and by thin disordered graphite layers at the ZrO_2/ZrO_2 boundaries.

Keywords: 3Y-TZP; Carbon nanofiber; Microstructure; Fracture; Electrical conductivity

1. Introduction

The discovery of carbon nanotubes (CNTs) has generated considerable interest owing to their small size, high aspect ratio, low mass and excellent mechanical, electrical and thermal properties.[1,2] As well as single-walled and multi-walled CNTs, there are similar carbon based filamentous nanomaterials/carbon nanostructures, e.g., carbon nanofibers with similar properties, but with slightly different sizes.[3] CNFs have cylindrical or conical structures that have diameters varying from a few to hundreds of nanometers and lengths ranging from less than a micron to millimeters. The internal structure of carbon nanofibers is comprised of different arrangements of modified graphene sheets, and the main distinguishing characteristic of nanofibers from nanotubes is the stacking of graphene sheets of varying shape.[4]

There are many potential applications of carbon based filamentous nanomaterials, which can be subdivided into two main categories. First as reinforcements in polymer, metallic and ceramic composites where they produce improved mechanical and functional properties.[5,6] These composites may find applications in catalyst supports, hydrogen storage, electrodes for fuel cells, supercapacitors and ultrafiltration membranes. The second category includes applications in which a single nanotube or nanofiber is used as an individual functional element, e.g., in field-emission displays, scanning probe tips and membranes for microfluidic devices and nanoelectronic devices.[4]

In the last few years new ceramic/carbon nanotube composites have been developed and a number of authors have reported improved mechanical and functional properties in the case of ceramic/CNT composites compared to the monolithic material.[7–11] Three main problems have been recognized during these investigations; dispersion of the CNTs in the matrix,[12] densification of the composites and degradation of the CNTs. Conventional mixing of CNTs with the matrix powder requires long milling times which may damage the CNTs. Alternative

* Corresponding author. Tel.: +421 55 79 22 462; fax +421 55 79 22 408.
E-mail address: jdusza@imr.saske.sk (J. Dusza).

0955-2219/$ – see front matter © 2009 Elsevier Ltd. All rights reserved.
doi:10.1016/j.jeurceramsoc.2009.05.030

processing routes have been investigated that result in better dispersions and reduced damage of CNTs. These include in situ growth of CNTs during the processing or ceramic synthesis in situ on CNTs.[13,14] Regarding the densification of the composites, authors have mainly used hot pressing (HP) or spark plasma sintering (SPS). Hot pressing often results in incomplete densification because the CNTs inhibit the densification, especially at higher volume fraction of CNTs. It has been reported that using SPS improves densification.[8,15]

The investigations to date have focused mainly on alumina based ceramic composites with only limited work on other systems, e.g., silicon nitride or zirconia.[16–18] Also, the reinforcing elements have mainly been CNTs and only a few investigations have involved CNFs. Therefore the potential advantages of CNFs compared to CNTs (price, shape, morphology) as reinforcing elements are still largely unexplored. Only in the last few years publications have appeared that illustrate the positive effect of carbon nanofibers as reinforcing elements in alumina, silicon carbide and hydroxyapatite based composites.[19–21]

Zirconia (3Y-TZP) is a material extensively used for many structural applications due to its good mechanical properties. Zirconia and/or zirconia based composites are interesting multifunctional materials for applications such as solid-oxide fuel cells, oxygen sensors and ceramic membranes because of their good ionic conductivity, high-temperature stability, high electrical breakdown field and large bandgap energy.[22]

The aim of the present contribution is to investigate the influence of the two different sintering routes and carbon nanofiber addition on the microstructure, mechanical and electrical properties of zirconia/carbon nanofiber composites.

2. Experimental procedure

The zirconia used was 3 mol.% Y-TZP (from Tosoh, Japan), which is well characterized with good mechanical properties. At room temperature it is an electrical insulator. Carbon nanofibers grade HTF150FF (Electrovac, Austria) were used. The manufacturer's specifications state that these CNFs have a diameter of 80–150 nm, specific surface area in a range of 20–100 m^2/g, Young's modulus of ~500 GPa, tensile strength of ~7 GPa and electrical resistivity of 10^{-3}–10^{-4} Ω cm.

The CNFs were dispersed by milling in Millipore water with dodecylbenzenesulfonic acid (DBSA) as a dispersing agent which was pre-mixed in the water before adding the CNFs. After adding the CNFs the mixture was ultrasonically dispersed for 10 min using a probe. Separately Y-TZP powder was also ball milled in Millipore water. The CNFs solution was added to the ceramic slip, and the mixture was then given a further ultrasonic treatment. This slip was continuously stirred and spray dried in a small laboratory spray dryer (model 190, Büchi, Germany). Composite powders were prepared with 2.0 and 3.3 vol.% CNF content.

The resultant powder granulates were die pressed into 20 mm diameter discs for hot pressing. These samples were hot pressed in an argon atmosphere at a dwell temperature 1300 °C for 30 min at a pressure of 41 MPa. For comparison monolithic ZrO_2 was prepared under similar conditions, e.g., hot pressed at 1300 °C for 30 min at a pressure of 41 MPa. For SPS, discs of 20 and 30 mm diameter were prepared. The SPS samples were sintered at different dwell temperatures. The samples with 2.0 vol.% CNFs were sintered at 1400 °C and the samples with 3.3 vol.% CNFs were sintered at 1500 °C in both cases for with a 5 min dwell time and at 60 MPa.

The CNFs were characterized by scanning and transmission electron microscopy (SEM, TEM, Jeol Ltd.). HREM using an TECNAI G^2 FEG SuperTWINN (200 kV) transmission-scanning electron microscope equipped with both side-entry wide angle SIS and on-axis bottom mounted Gatan 2K CCD cameras. The local chemical analysis was measured with an integrated X-ray energy dispersive attachment (EDS) with a EDAX UTW detector. The density of the experimental materials was measured using the Archimedes method. XRD analysis (Phillips, X-pert) was used to determinate the phase composition of the experimental materials. In order to provide information on chemical composition and carbon bonding, the samples were examined by XPS and XAES methods using a VG ESCA3 MkII electron spectrometer. The spectra were recorded with Al Kα radiation and an electrostatic hemispherical analyzer operated in the fixed analyzer transmission mode.

Specimens for microstructure examination were prepared by diamond cutting, grinding, polishing and thermal etching at a temperature of 1250 °C in air and carbon coated before the examination. The average grain size of the zirconia matrix grains of the monolithic and composites were measured using the standard line intercept technique from SEM micrographs of thermally etched polished surfaces.[23] For TEM thin foils were prepared using a focused ion beam (Quanta 3D system).

The microhardness (Leco instruments) and hardness were measured using the Vickers indentation method at loads from 0.25 to 150 N. The small specimen size did not allow use of standard fracture toughness tests, therefore indentation fracture toughness testing was performed at loads of 50 and 100 N using a Vickers indenter, and the calculation were made using the Shetty et al. equation.[24] Microfractography was used to analyse the fracture lines and surfaces of the specimens to study the fracture micromechanisms in the monolithic material and in the composites. The electrical conductivity (resistivity) was measured at room temperature using a four point method. Specimens with the dimension of 1.5 mm × 1.5 mm × 10 mm were cut from the centre of the hot pressed samples for these measurements.

3. Results and discussion

3.1. Microstructure characterisation

The SEM and TEM analyses revealed that the outer diameter of the nanofibers varied from 50 to 600 nm and the length of the fibers varied from several micrometers to several tens of micrometers. Two type of fibers were identified; hollow pipe shaped and bamboo shaped fibers as shown in Fig. 1. The hollow pipe shaped fibers are usually defect free and consist of a distinct sandwich of graphite layers parallel to the fiber axes. The bamboo shaped fibers (which are less than 5% by volume) often contain defects at the nano-level, and their walls are built from

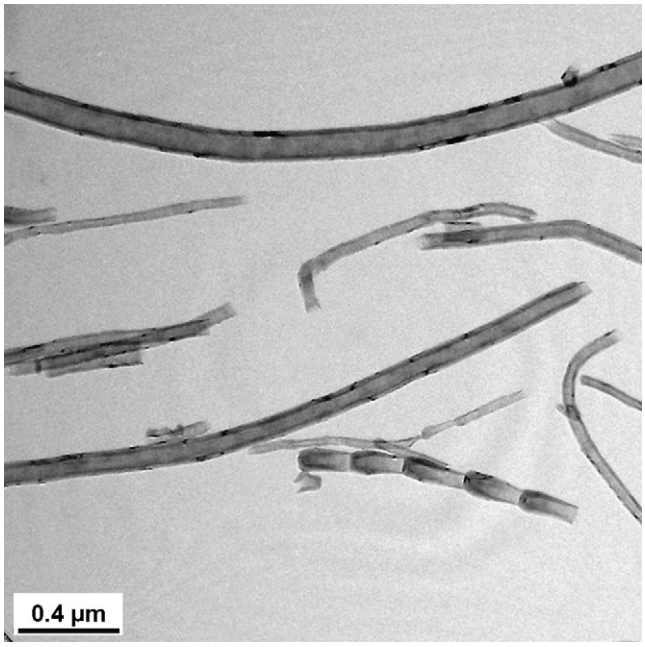

Fig. 1. Characteristic shapes of the carbon nanofibers, TEM.

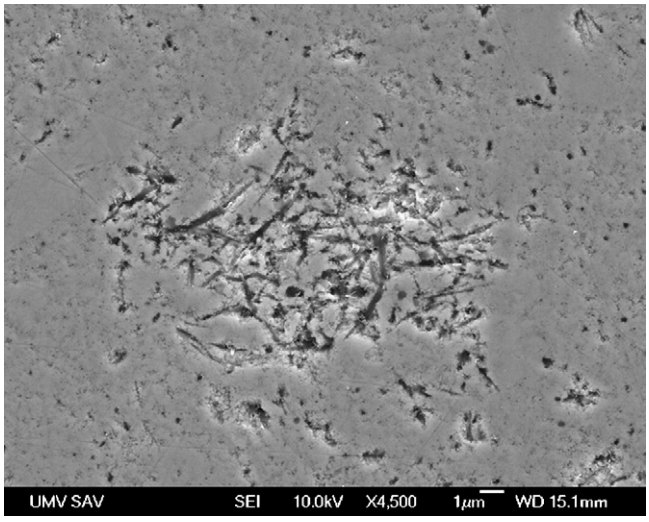

Fig. 3. Defects in the form of clusters of CNFs on polished surface of the HP composite.

domains with different orientation of graphite layers. The fibers contain 99.05 at.% carbon and 0.95 at.% oxygen with a binding energy of O (1s) electrons of 532.7 eV, which corresponds the C–O bond.[25] Clusters of CNFs have been identified in the CNF powder in the form of hard agglomerates, Fig. 2.

The hot pressed monolithic zirconia was fully dense but the ZrO2–CNF composites contained porosity, which was associated with clustering of the carbon nanofibers. Relatively large numbers of CNF clusters were observed on the polished and fracture surfaces of the composites (e.g., in Fig. 3). The size of the clusters varied from a few microns up to approximately 40 μm, and porosity was always associated with these clusters. As expected the volume fraction of the clusters was higher in the composites with the higher CNF starting content. The presence of such clusters and the associated porosity is the main reason of the lower density of the composites compared to their theoretical density. There is a good correlation between the measured density and the presence of clusters/porosity in the two composites processed by different routes. The addition of CNFs to the zirconia has a significant effect on the sintering behavior of zirconia. This is not in accordance with the results of Zhan et al.[16,26] who found that addition of 3 vol.% of CNTs to an alumina matrix had no effect on the sintering process and the density of the composite was almost the same as pure alumina. Similarly Sun et al. and Ukai et al.[10,11] presented almost full density for zirconia–CNTs composites with up to 1 wt.% CNTs prepared by hot isostatic pressing and SPS. These results may indicate that the ceramic–CNT composites sinter more easily compared to the ceramic–CNF composite. However recently Maensiri et al.[19] developed hot-pressed alumina based composites reinforced with up to 5 vol.% CNF with very similar dimensions of the nanofibers as was used in the present investigation, and found almost theoretical density for his materials. From this it seems that either the sintering of the zirconia based composite is principally more difficult compared to the sintering of alumina–CNF system or the processing technique in the present investigation has to be improved.

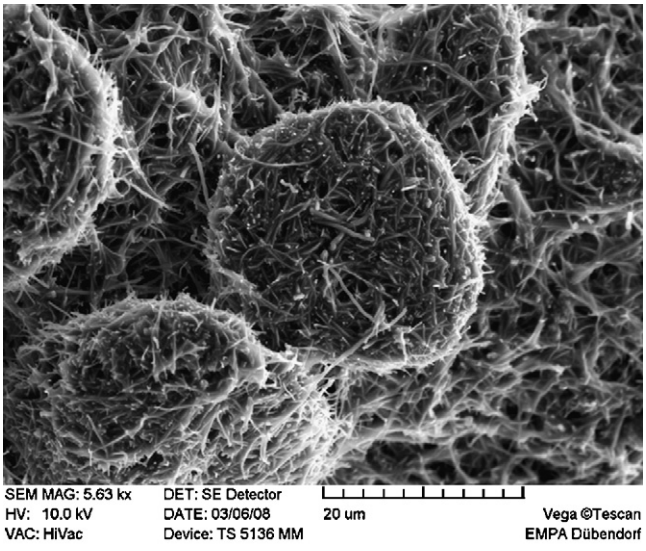

Fig. 2. Agglomerates of CNFs in the powder.

In Fig. 4 the microstructure of the HP monolithic zirconia and the HP ZrO_2–2.0 vol.% CNF composite is illustrated at a lower magnification. The monolithic zirconia consists of submicron/nanometer sized grains with randomly occurring defects in the form of pores with dimensions of approximately 100–200 nm (Fig. 4a). The microstructure of the composite consists of a similar or an even smaller grained matrix with relatively well dispersed CNFs in the matrix, the locations of the burned out CNFs during the thermal etching are shown in Fig. 4b.

The detailed microstructure of the monolithic zirconia and the zirconia matrix of the composites are illustrated in Fig. 5a and b. The average grain size of the monolithic material is 160 nm and in the composites it is smaller and varies from 95 to 135 nm.

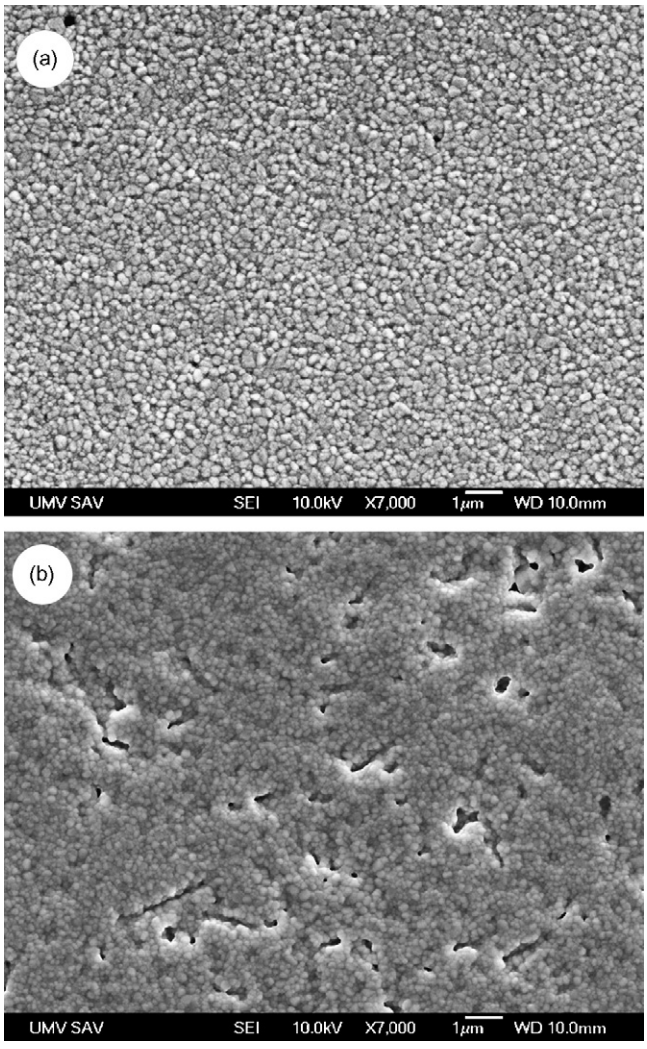

Fig. 4. Microstructure of the HP monolithic zirconia (a) and HP ZrO_2 + 2 vol.% CNFs composite at low magnification, thermally etched (b).

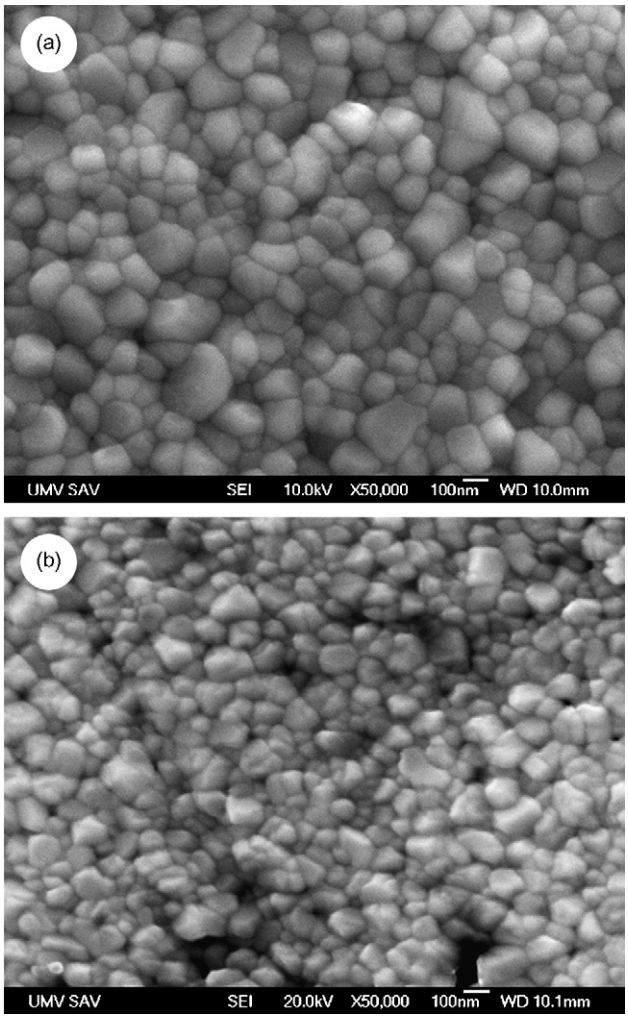

Fig. 5. Microstructure of the matrix in HP (a) and SPS (b) ZrO_2 + 2 vol.% CNFs composite.

The smaller grain size of the zirconia in the composites compared to the monolithic material is evidence that the CNFs hinder the grain growth in the composite during sintering. The slightly smaller grained matrix in the composites sintered by SPS is explained by a shorter sintering time compared to the HP regime.

In monolithic zirconia the grain boundaries were clean interphases between two ZrO_2 grains with no secondary phase. In the composites beside these grain boundaries we found two other types of boundaries illustrated in Fig. 6a and b. The first was a ZrO_2/ZrO_2 boundary with a carbon nanofiber with a diameter of approximately 20 nm (Fig. 6a) and the second (Fig. 6b) a ZrO_2/ZrO_2 boundary with disordered graphite, resulting from the degradation of CNFs during the powder preparation and the sintering routes.

3.2. Mechanical and fracture properties

In Table 1 the basic properties such as the density, hardness and indentation toughness are presented for the monolithic zirconia and for the HP and SPS composites. The hardness of all of the composites (with both volume fraction of CNFs and prepared by HP or SPS) is significantly lower compared to the hardness of the monolithic material. The hardness of the SPS materials is higher at both CNF volume fractions compared to the hardness of the HP composites which is in a good correlation with the measured densities. The indentation toughness decreased after addition of CNFs to the zirconia except for the SPS composite with 2.0 vol.% of CNFs where a slight improvement has been found (Fig. 7).

The fracture mechanisms in the bulk zirconia material are mainly intergranular with a very low roughness of the fracture lines/surface, only apparent at the nanometer scale. No toughening mechanisms have been revealed on the fracture lines/surfaces in this system in the form of frictional or mechanical interlocking of the grains because of the very small grain size. The composites reinforced by CNFs exhibit a slightly different behavior with more rough fracture line/surfaces with crack deflection at the larger singular CNFs. The crack deflection is similar to the crack deflection in whisker reinforced ceramics and represents one of the toughening mechanisms in similar systems that can improve the fracture toughness of the composites. Beside the crack deflection (Fig. 8a), crack bridging and CNF pull-out

Table 1
Properties of the investigated materials.

System	Density (g/cm^3)	HV_1 (kg/mm^2)	K_{Indent} (MP am$^{0.5}$)	Electrical conductivity (S/m)
ZrO_2HP	6.05	1400 ± 28	6.24 ± 0.1	–
ZrO_2 + 2.0% CNF-HP	5.2	820 ± 30	5.5 ± 0.17	630 ± 149
ZrO_2 + 3.3% CNF-HP	5.0	654 ± 25	4,75 ± 0.24	983 ± 200
ZrO_2 + 2.0% CNF-SPS	5.68	968 ± 42	6.4 ± 0.42	391 ± 117
ZrO_2 + 3.3% CNF-SPS	5.52	802 ± 38	5.2 ± 0.35	813 ± 273

(Fig. 8b and c) was often detected on the fracture surface of the failed composite, however the pull-out length were usually short (Fig. 8a and b). Based on the fractographic examination it seems that the toughening mechanisms by CNFs were more effective in the SPS materials, which is probably the reason of the higher indentation toughness of SPS composites.

Recently CNFs have been used for improving the mechanical properties of different ceramics. Maensiri et al.[19] used similar CNFs as in the present investigation and found that the influence of the CNFs addition on the mechanical properties of the alumina–CNF composites is similar to that found in our investigation for zirconia–CNF composite. They found an improvement in the fracture toughness of approximately 13% with a volume fraction of CNFs of 2.5 vol.% but the hardness and bending strength decreased with increasing volume fraction of CNFs. Hirota et al.[20] synthesized and consolidated CNF reinforced SiC from a mixture of Si, amorphous C and B powders and CNFs using SPS processing. For the composites with 5–15 vol.% of CNFs they achieved 96% of theoretical density, and for the system with 10 vol.% of CNFs very high mechanical properties: bending strength of 700 MPa, hardness of 26 GPa and fracture toughness of 5.5 MPa m$^{0.5}$.

The lower hardness of the composite compared to the monolithic material is mainly dependent on the residual porosity that remains in the material after the sintering, similar to that observed in other investigations.[10] Together with the porosity, the clusters of the CNFs/CNTs are characteristic processing defects present in our material and presented in all of the work dealing with similar composites. This indicates the still present difficulties in the preparation of defect free carbon nanotubes or carbon nanofibers reinforced ceramic composites but also the potential for the improvement of their functional and mechanical properties.

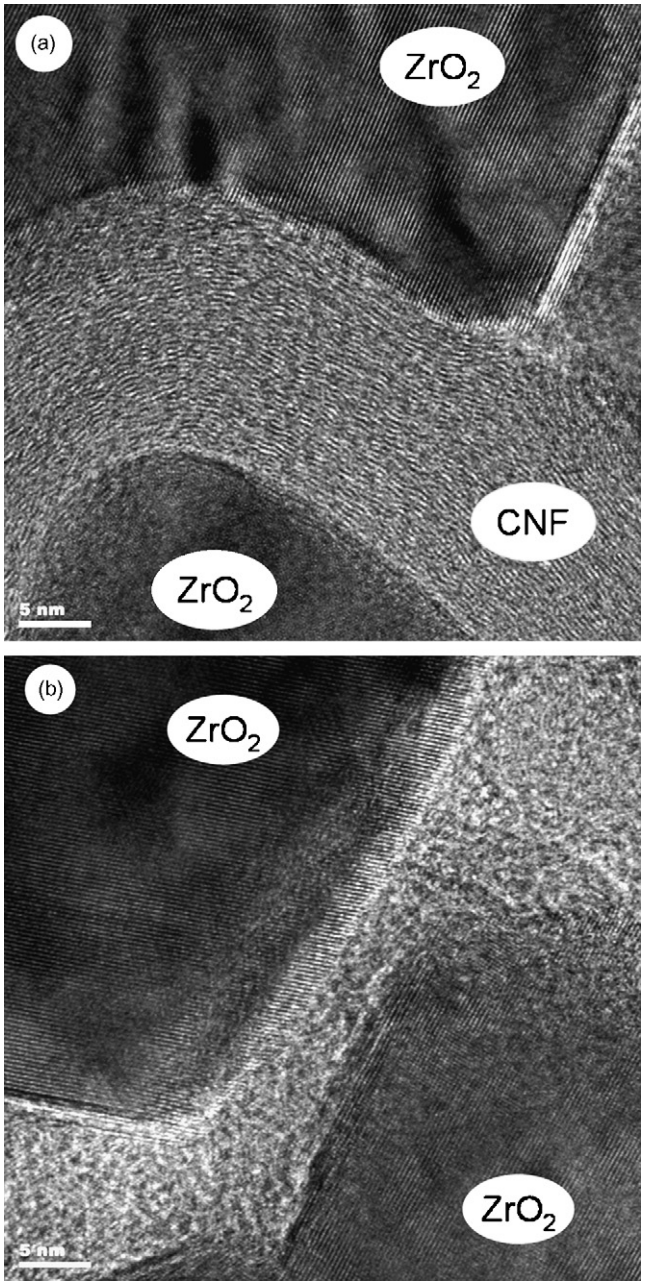

Fig. 6. Grain boundaries ZrO_2/ZrO_2 in HP composite with a CNF at the interphase (a) and with a disordered graphite at the interphase, (b).

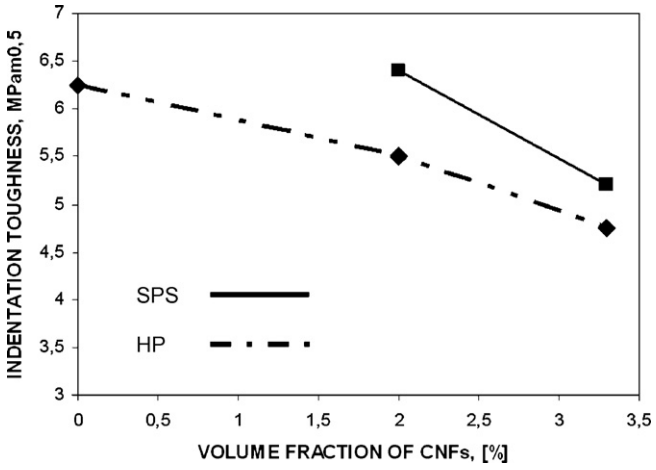

Fig. 7. Influence of the volume fraction of CNFs on the indentation toughness.

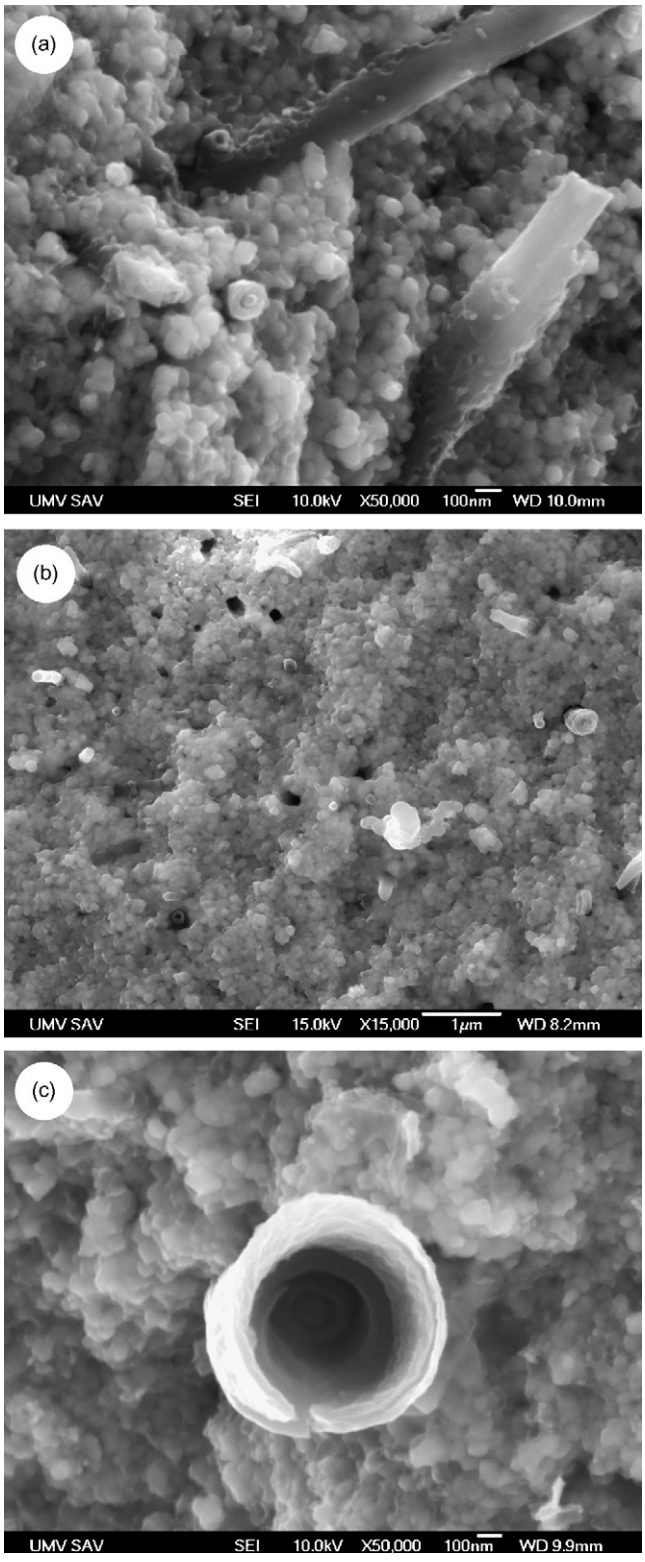

Fig. 8. Fracture surface of HP (a and c) and SPS (b). CNF/zirconia composites illustrating the crack deflection at CNFs (a) and CNFs pull-out (b and c).

Similarly, as in the present contribution many authors[10,11] used the indentation technique for the toughness measurements, which is useful only for comparison purposes, but cannot be considered a true material property and also tends to over estimate the K_{Ic} value as described by Quinn and Brandt.[30] In several investigations more standard testing methods were applied for the measuement of fracture toughness of ceramic–CNT/CNF composites, e.g., in the works of Ye et al.[31] and Wei et al.[32] There is however another problem, they used the single-edge notched beam method but with a notch width of approximately 0.2 mm, which may have resulted in a measured fracture toughness that overestimated the true fracture toughness of the materials. In these investigations and the current study a more reliable technique (e.g., SEVNB[33]) has to be used for the measurement of the fracture toughness on fully dense composites to obtain information concerning the true effect of the CNFs on the fracture toughness.

As regards the fracture toughness, our results show that even the use of relatively coarse whisker like CNFs is not effective in toughening a zirconia ceramic matrix at the volumes used. On the other hand we have to note that on the fracture surface/line we frequently found different toughening mechanisms, mainly in the form of crack deflection at the CNFs and pull-out of CNFs. The reason for the relatively low indentation toughness is probably the poor dispersion and therefore the limited toughening effect of the CNFs. An interesting comparison between the carbon nanotube (CNT) and carbon nanofiber reinforcements in silicon nitride coatings has been published more recently[30] and the effectiveness of these reinforcements as toughening agents was compared by examining the fiber pull-out length from fracture surfaces. Their results provide an important insight into the relationship between the structure of the toughening agent and toughening mechanisms at the nano scale. They found that the hollow concentric graphitic MWNTs results in much longer pull-out lengths compared to the behavior observed in the case of solid core carbon nanofibers, which is in agreement with previous theories.[33] The carbon nanofibers used in the present investigation are coarser compared to the nanotubes in the experiment of Kothari et al.[29] The hollow or bamboo-shaped nanofibers used in the current study have similar graphitic structure as the MWCNTs used in[30] and can act as a toughening agent in a similar way. As has already been mentioned, a very important issue for toughening in fiber-reinforced composites is the nature of the interface between fiber and the matrix, which must be of sufficiently low toughness to debond and be able to slide with friction. According to Xia et al.[33] the lack of molecular-scale perfection in nanotubes may provide some benefit in the toughening process. Ideal MWCNTs may exhibit extremely easy inter-wall sliding that prevents toughening behavior because of the easy telescoping of inner walls from outer walls. Imperfect nanotubes or nanofibers may provide more effective load transfer from outer to inner walls, resulting in enhanced toughness and strength. It seems that from the point of view of toughening there are two important interfaces; the outer between the CNTs/CNFs and the ceramic matrix and the internal between the individual graphite layers of the CNTs/CNFs. The first has to be designed during the processing of the composite, the second during the preparation of the CNTs and CNFs. However, we have to note that the toughening mechanism connected with the internal interface can be effective in the case of cylindrical hollow CNFs only (Fig. 8c), and not in the case of bamboo-shaped CNFs, partially used in the present experiment.

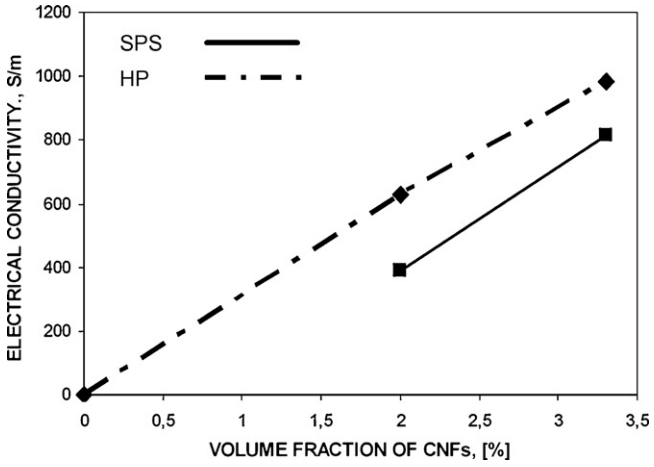

Fig. 9. Influence of the volume fraction of CNFs on the electrical conductivity.

3.3. Electrical properties

In Table 1 and Fig. 9 the electrical conductivity of the investigated materials is presented. The electrical conductivity increased significantly from a very low value (it was not possible to measure the exact value of the zirconia because of the limitations of our measurement equipment) to the maximum value of 985 S/m for the HP composite with 3.3 vol.% of CNFs. The electrical conductivity of the HP composites in all cases, is higher compared to that of the SPS materials, Fig. 9. This is surprising considering the higher density of the SPS composites in comparison to HP composites.

The thermoelectric properties of 10 vol.% single-wall carbon nanotube/3Y-TZP nanocomposite produced by SPS have been studied by Zhan and Mukherjee.[6] Two types of CNTs were used; purified with more than 90% of the catalyst particles removed and unpurified. The CNTs were distributed and entangled within the ceramic matrix with some degree of agglomeration and the matrix was in the nanocrystalline range, hence, similar to the materials in the present investigation. According to these results, the electrical conductivity decreased from approximately 500 to approximately 200 S/m when the temperature increased from room temperature to 550 K. A further increase of the testing temperature resulted in a slight increase of electrical conductivity. Shi and Liang studied the effect of the MWCNT addition on the electrical and dielectric properties of MWCNT/3Y-TZP composite prepared by SPS.[27] The CNTs that they used typically consisted of 8–15 graphite layers around the hollow 5 nm core, with diameters from 20 to 40 nm and lengths from 0.05 to 0.5 μm. The granular grains of the matrix were less than 1 μm in size, and randomly orientated and agglomerated CNTs were also found. They found a very strong influence of the CNT addition on the electrical conductivity of the composite in the range of 1–2 wt.% of CNTs. MWCNT/3Y-TZP composites have been prepared by pressureless sintering + HIP by Ukai et al.[11] For the materials with wt.% of CNTs from 0.25 to 1.0 the electrical conductivity was found to be in the range of 5–60 S/m which is lower than our results and indicate the potential of the nanofibers for improving the functionality of the ceramics.

It was found that the ZrO_2/2.0 vol.% CNF composite investigated in the present study exhibits very good electrical conductivity of 630 S/m which can be explained by the change in the grain boundaries in the composite compared to the monolithic zirconia. It seems however, that the increased conductivity of the composites is not only produced by the CNFs in their original form, but also the disordered graphite phases at the ZrO_2/ZrO_2 boundaries. Fényi et al.[28] investigated the influence of the CNT, black-carbon (BC) and graphite (GR) addition on the electrical conductivity of Si_3N_4. It was found that the size and shape of the mixed graphite additives resulted in a very limited graphite grain connection in the matrix, which resulted in the lowest electrical conductivity of the composite prepared using this additive. The composite with the highest conductivity produced with carbon black additions owing to their nano size producing bunchy, chainy cluster forms in the pores and on the surface of the matrix grains. In the case of CNT additions, significant improvement of electrical conductivity up to approximately 700 S/m was achieved. In our case the nano-sized graphite in the form of a thin layer at the ZrO_2 boundaries with a width of approximately 10 nm can create even at a low volume fraction a percolation network through the material (together with the CNFs) which significantly increased the electrical conductivity.

Our future work will follow two aims: to improve the processing route to produce fully dense composites with improved dispersion of the CNFs, and to fully understand the role of the CNFs in changing the electrical, thermal and mechanical properties of the zirconia–CNFs composite.

4. Conclusions

Zirconia/Carbon nanofiber composites with different volume fraction of carbon nanofibers have been processed using two different routes: hot pressing and spark plasma sintering. The main conclusions are as follows:

- The presence of the CNFs makes densification more difficult. As regards the density the spark plasma sintering is more effective in sintering the composites compared to the hot pressing;
- The grain growth in composites is suppressed by the CNFs, which results in a very fine nanocrystalline zirconia matrix;
- Clusters of CNFs together with porosity are present in the composites as a result of the difficulty of dispersing the ceramic/CNFs mixture;
- The hardness and indentation toughness (except SPS ZrO_2 +2.0 vol.% CNFs) of the composites are lower compared to the monolithic zirconia due to the presence of pores and clusters. However, a potential for toughening by CNFs has been recognized;
- The composites exhibit significantly higher electrical conductivity compared to the monolithic material due to the presence of CNFs and a change at the ZrO_2/ZrO_2 grain boundaries.

Acknowledgements

The experimental material was partly prepared by Chintan Shah and Annamary Duszova. Further, the authors would like to thank Izabel Silveira, for the help with dispersion of the CNT, XRD measurement and electrical conductivity measurements, respectively. The work was supported by NANOSMART, Centre of Excellence, SAS, by the Slovak Grant Agency for Science, grant no. 2/7914/27 by the APVV 0171-06 and LPP 0203-07, LPP0174-07 and by the KMM-NoE EU 6FP Project. We would also like to acknowledge the assistance of Nanoforce Technology Limited with the SPS processing and the financial support of RUAG Components, Altdorf, Switzerland.

References

1. Iijima, S., Helical microtubules of graphitic carbon. *Nature*, 1991, **354**, 56.
2. Arben Merkoci, Carbon nanotubes in analytical sciences. *Microchim. Acta*, 2006, **152**, 157–174.
3. Uchida, T., Anderson, P. D., Minus, M. L. and Kumar, S., Morphology and modulus of vapor grown carbon nano fibers. *J. Mater. Sci.*, 2006, **41**, 5851–5856.
4. Melechko, A. V., Merkulov, V. I., McKnight, T. E., Guillorn, M. A., Klein, K. L., Lowndes, D. H. and Simpson, M. L., Vertically aligned carbon nanofibers and related structures: Controlled synthesis and directed assembly. *J. Appl. Phys.*, 2005, **97**, 041301.
5. Laurent, Ch., Peigney, A., Dumortier, O. and Rousset, A., Carbon nanotubes-Fe-alumina nanocomposites. Part II: microstructure and mechanical properties of the hot-pressed composites. *J. Eur. Ceram. Soc.*, 1998, **18**, 2005.
6. Zhan, G. D. and Mukherjee, A. K., Carbon nanotube reinforced alumina based ceramics with novel mechanical, electrical and thermal properties. *J. Appl. Ceram. Technol.*, 2004, **1**(2), 161.
7. Zhan, G. D., Kuntz, J. D., Garay, J. E., Mukherjee, A. K., Zhu, P. and Koumoto, K., Thermoelectric properties of carbon nanotube/ceramic nanocomposites. *Scripta Mater.*, 2006, **54**, 77–82.
8. Wang, X., Padture, N. P. and Tanaka, H., Contact damage-resistant ceramic/single wall carbon nanotubes and ceramic/graphite composites. *Nat. Mater.*, 2004, **3**, 539–544.
9. Peigney, A., Rul, S., Lefevre-Schick, F. and Laurent, C., Densification during hot-pressing of carbon nanotube-metal-magnesium aluminate spinel nanocomposites. *J. Eur. Ceram. Soc.*, 2007, **27**, 2183.
10. Sun, J., Gao, L., Iwasa, M., Nakayama, T. and Niihara, K., Failure investigation of carbon nanotube/3Y-TZP nanocomposites. *Ceram. Int.*, 2005, **31**, 1131–1134.
11. Ukai, T., Sekino, T., Hirvonen, A., Tanaka, N., Kusunose, T., Nakayama, T. and Niihara, K., Preparation and electrical properties of carbon nanotubes dispersed zirconia nanocomposites. *Key Eng. Mater.*, 2006, **317–318**, 661–664.
12. Inam, F., Yan, H., Reece, M. J. and Peijs, T., Dimethylformamide: an effective dispersant for making ceramic-carbon nanotube composites. *Nanotechnology*, 2008, **19**, 195710.
13. An, J. W., You, D. H. and Lim, D. S., Tribological properties of hot-pressed alumina-CNT composites. *Wear*, 2003, **255**, 677–681.
14. Liu, Y. Q. and Gao, L., A study of the electrical properties nanotube–$NiFe_2O_4$ composites: effect of the surface treatment of the carbon nanotubes. *Carbon*, 2005, **43**, 47–52.
15. Zhan, G. D., Kuntz, J. D., Garay, J. E. and Mukherjee, A. K., Electrical properties of nanoceramics reinforced with ropes of single-walled carbon nanotubes. *Appl. Phys. Lett.*, 2003, **83**, 1228–1230.
16. Zhan, G. D., Kuntz, J. D., Wan, J. and Mukherjee, A. K., Single-wall carbon nanotubes as attractive toughening agents in alumina based nanocomposites. *Nat. Mater.*, 2003, **61**, 1899.
17. Balazsi, Cs., Kónya, Z., Wéber, F., Biró, L. P. and Arató, P., Preparation and characterization of carbon nanotube reinforced silicon nitride composites. *Mat. Sci. Eng. C*, 2003, **23**, 1133–1137.
18. Tatami, J., Katashima, T., Komeya, K., Meguro, T. and Wakihara, T., Electrically conductive CNT-dispersed silicon nitride ceramics. *J. Am. Ceram. Soc.*, 2005, **88**, 2889.
19. Maensiri, S., Laokul, P., Klinkaewnarong, J. and Amornkitbamrung, V., Carbon nanofiber-reinforced alumina nanocomposites: Fabrication and mechanical properties. *Mater. Sci. Eng. A*, 2007, **447**, 44–50.
20. Hirota, K., Hara, H. and Kato, M., Mechanical properties of simultaneously synthesized and consolidated carbon nanofiber (CNF)-dispersed SiC composites by pulsed electric-current pressure sintering. *Mater. Sci. Eng. A*, 2007, **458**, 216–225.
21. Kobayashi, S. and Kawai, W., Development of carbon nanofiber reinforced hydroxyapatite with enhanced mechanical properties. *Composites: Part A*, 2007, **38**, 114–123.
22. Lee, S. Y., Kim, H., McIntyre, P. C., Saraswat, K. C. and Byun, J. S., Atomic layer deposition of ZrO_2 on W for metal–insulator–metal capacitor application. *Appl. Phys. Lett.*, 2003, **82**, 2874–2876.
23. ASTM, *Standard Test Methods for Determining Average Grain Size*., 1996, p. 243 [E112-96].
24. Shetty, D. K., Wright, I. G., Mincer, P. N. and Clauser, A. H., Indentation fracture of WC-Co cermets. *J. Mater. Sci.*, 1985, **20**, 1873–1882.
25. Dusza, J., Morgiel, J., Bastl, Z., Švec, P., Tatarko, P. and Puchy, V., Characterization of Carbon Nanofibers. Carbon Int. J., submitted for publication.
26. Wei, T., Fan, Z., Luo, G. and Wei, F., A new structure for multi-walled carbon nanotubes reinforced alumina nanocomposite with high strength and toughness. *Mater. Lett.*, 2008, **62**, 641–644.
27. Shi, S.-l. and Liang, J., Effect of multiwall carbon nanotubes on electrical and dielectric properties of yttria-stabilized zirconia ceramic. *J. Am. Ceram. Soc.*, 2006, **89**(11), 3533–3535.
28. Fényi, B., Arató, P., Wéber, F., Hegman, N. and Balázsi, Cs., Electrical examination of silicon nitride–carbon composites. *Mater. Sci. Forum*, 2008, **589**, 203–208.
29. Kothari, A. K., Jian, K., Rankin, J. and Sheldon, B. W., Comparison between carbon nanotube and carbon nanofiber reinforcements in amorphous silicon nitride coatings. *J. Am. Ceram. Soc.*, 2008, 1–4.
30. Quinn, G. D. and Brandt, R. C., On the Vickers indentation fracture toughness test. *J. Am. Ceram. Soc.*, 2007, **90**, 673–680.
31. Ye, F., Liu, L., Wang, Y., Zhou, Y., Peng, B. and Meng, Q., Preparation and mechanical properties of carbon nanotube reinforced barium aluminosilicate glass–ceramic composites. *Scripta Mater.*, 2006, **55**, 911–914.
32. Wei, T., Fan, Z., Luo, G., Wei, F., Zhao, D. and Fan, J., Preparation and mechanical properties of carbon nanotube reinforced barium aluminosilicate glass-ceramic composites. *Mater. Res. Bull.*, 2008, **43**, 2806–2809.
33. Kübler, J., *Fracture Toughness of Ceramics using the SEVNB Method: From a Preliminary Study to a Standard Test Method, Fracture Resistance Testing of Monolithic and Composite Brittle Materials*, ASTM STP 1409, ed. J. A. Salem, M. G. Jenkins, and G. D. Quinn. ASTM, West Conshohocken, PA, USA, ISBN 0-8031-2880-0, January 2002, pp. 93–106.